



Contents lists available at ScienceDirect

Arabian Journal of Chemistry

journal homepage: www.ksu.edu.sa

Original article



Novel thiazole-derived Schiff-Bases as efficient corrosion inhibitors for mild steel in acidic Media: Synthesis, electrochemical and Computational insights

Nizar El Guesmi^{a,b,*}, Basim H. Asghar^{a,*}, Mohamed I. Awad^{a,c}, Abdulrahman N. Al Harbi^a, Mohammed A. Kassem^{a,d}, Mohamed R. Shaaban^{a,c}

^a Department of Chemistry, Faculty of Science, Umm Al-Qura University, Makkah, Saudi Arabia

^b Department of Chemistry, Faculty of Science, Monastir University, Monastir, Tunisia

^c Department of Chemistry, Faculty of Science, Cairo University, Giza, Egypt

^d Department of Chemistry, Faculty of Science, Benha University, Benha, Egypt

ARTICLE INFO

Keywords:

Thiazole-derived Schiff-Bases
Corrosion Inhibitors
Electrochemical Measurements
Mild Steel
Quantum Chemical Calculation

ABSTRACT

Novel thiazole-derived Schiff bases **3a-c** have been synthesized via thermal as well as microwave assisted condensation of 2,4-dihydroxybenzaldehyde and aminothiazole derivatives in an ethanolic solution containing catalytic amounts of acetic acid. The structure of the synthesized thiazole-based Schiff bases was elucidated by spectroscopic tools as well as their elemental analyses. The efficiency of these compounds in corrosion inhibition was evaluated for mild steel in H₂SO₄ solution using electrochemical techniques. Studying the behavior of these compounds under various conditions clarified their effectiveness as beneficial corrosion inhibitors. Increasing the concentration of both inhibitors led to higher effectiveness in inhibiting corrosion. The inhibition efficiency (IE) of studied inhibitors was found to increase in the following order; **3c** > **3b** > **3a**. The mechanism of adsorption was suggested based on the Temkin adsorption isotherm, and was found to follow mixed mode of adsorption, with the chemical mode is the prevailing as revealed from the free energy change values. Moreover, the correlation between the inhibition efficiency and the molecular structure of the examined inhibitors was explored through quantum chemical calculations. These calculations demonstrated that the high electron density on the Schiff bases molecule contributes to a high corrosion inhibition efficiency. Additionally, the addition of an electron donor group on the thiazole ring enhanced the molecule's adsorption ability on the mild steel surface.

1. Introduction

The imine or azomethine functionality in Schiff bases is one of the most widely used building blocks for molecules characterized by interesting physical and chemical properties. Additionally, they participate in biologically significant reactions and are extensively utilized in the formation of metal complexes.

(More et al., 2019; Li et al., 2019; Berhanu et al., 2019; Long, 2019; Alzahrani et al., 2023; Mahadevi and Sumathi, 2020; Alorini et al., 2022; Abdalla et al., 2022; Kaur et al., 2021; Uddin et al., 2020; Ahmed et al., 2019; Verma and Quraishi, 2021).

Moreover, Schiff bases are a widely studied class of chemical compounds known for their anticorrosive properties. (Al-Amiery et al., 2022; Abdel-karim et al., 2024; Betti et al., 2023; Kamal et al., 2022;

Khanna et al., 2024; Altalhi, 2023; Abd-elmaksoud et al., 2023; Fouda et al., 2023; Chugh et al., 2020; Verma and Quraishi, 2021; Abdelsalam et al., 2022; Yurt et al., 2014; Pour-Ali et al., 2023; Pour-Ali and Hejazi, 2022). The mechanism of action involves the > C = N- (imine) group adsorbing onto the metallic surface. The substituents' ability in the molecule to donate or withdraw electrons significantly influences the adsorption and binding affinity of Schiff bases to metallic surfaces.

The ability of organic compounds as corrosion inhibitors is enhanced by substituents of electron-donating characteristics (such as -NMe₂, -NH₂, -OR, -OH, and -SH, etc.). It has been reported that Schiff bases with polar substituents in specific positions can enhance chelation ability with metal ions (Verma and Quraishi, 2021). Therefore, these Schiff bases act as stronger ligands or corrosion inhibitors as compared with unsubstituted counterparts. In interactions between such

* Corresponding authors.

E-mail addresses: naguesmi@uqu.edu.sa (N. El Guesmi), bhasghar@uqu.edu.sa (B.H. Asghar).

<https://doi.org/10.1016/j.arabjc.2024.105867>

Received 2 March 2024; Accepted 9 June 2024

Available online 10 June 2024

1878-5352/© 2024 The Authors. Published by Elsevier B.V. on behalf of King Saud University. This is an open access article under the CC BY-NC-ND license (<http://creativecommons.org/licenses/by-nc-nd/4.0/>).

Schiff bases and metallic atoms, both the imine $>C=N-$ and polar functional groups (such as $-OH$) act as electron donor sites.

Many heterocyclic compounds containing aromatic systems, π -bonds, and heteroatoms (such as N, S, and O) often demonstrate effective anticorrosion properties, attributed to their ability to bind to the metal surface through lone pairs of electrons and/or pi-electrons. (Al-Amiery et al., 2022; Betti et al., 2023; Khanna et al., 2024; Altalhi, 2023; Abd-elmaksoud et al., 2023; Chugh et al., 2020; Verma and Quraishi, 2021; Abdelsalam et al., 2022; Yurt et al., 2014; Hamani et al., 2014; Zhang et al., 2015).

In general, compounds containing both nitrogen and sulfur, such as thiazoles, have demonstrated higher effectiveness in inhibiting corrosion compared to those containing only one of these elements. Schiff bases, known for their corrosion inhibition properties, have been particularly effective. Therefore, Schiff bases of thiazoles have been developed and studied for their efficiency as corrosion inhibitors. (Chugh et al., 2020; Gong et al., 2019). Due to their aromatic rings containing nitrogen and sulfur atoms, thiazoles and their derivatives are widely recognized for their generally low toxicity.

(Gong et al., 2019). Recent theoretical calculations have provided a more comprehensive explanation of the inhibition mechanism of thiazoles and their derivatives. (Gong et al., 2019). A molecule is likely to demonstrate enhanced adsorption on an iron surface when it possesses a higher energy of HOMO (E_{HOMO}), a lower energy of LUMO (E_{LUMO}), and a lower energy difference between HOMO and LUMO (ΔE) (Gong et al., 2019; Abdallah et al., 2021a; Abdallah et al., 2021b; Guo et al., 2017; Xu et al., 2014; Arslan et al., 2009; Hegazy et al., 2013). Computational methods are employed based on density functional theory (DFT) to determine such parameters (Gong et al., 2019; Abdallah et al., 2021a; Abdallah et al., 2021b; Guo et al., 2017; Xu et al., 2014; Arslan et al., 2009; Hegazy et al., 2013; Hussein et al., 2020; El Guesmi et al., 2019; El Guesmi et al., 2017). The inhibition efficiency can be attributed to their low electronegativity and strong polarizability, which allow them to cover broad metal surfaces and rapidly transfer electrons to vacant atomic orbitals. Although various other Schiff bases have been reported in the literature, the corrosion inhibition efficacy of thiazole-derived Schiff bases has not been thoroughly explored using both experimental and theoretical methods.

Therefore, in the present work thiazole-derived Schiff bases **3a-c** have been synthesized and applied as a corrosion inhibitor for mild steel in acid medium. Potential dynamic polarization curves were used to study the corrosion inhibition of mild steel by molecules **3a-c** in 0.5 M H_2SO_4 solution. The adsorption abilities of **3a-c** on the iron surface were evaluated by performing quantum calculations to optimize the geometry and determine the energy of frontier molecular orbitals. The inclusion of three structurally relevant compounds in this study, both in practical and theoretical aspects, aims to standardize the corrosion process. This approach also aids in predicting corrosion inhibition methods, potentially leading to the development of highly efficient compounds. Schiff base have been reported as unique corrosion inhibitor in various media and in many applications. This wide range of applications is attributed to the structure which in addition to the main moiety, it includes both nitrogen and sulfur atoms, which each of which pertain inhibition efficiency in certain media. In addition, it is effective and ecofriendly solution for inhibiting metal corrosion with long term protection.

2. Experimental

2.1. Organic synthesis

2.1.1. Instruments and materials

Gallen-Kamp apparatus was used to determine melting points of the synthesized compounds. Distilled solvents were used and dried by using reported literature methods prior to their use. Microwave irradiation experiments were achieved using CEM machine of the model MARS system of which is a multi-mode platform. The machine is equipped with

a stirring plate which operates by a magnet and a rotor that permits the parallel processing of several vessels per run. The reaction vessel that was used is the Teflon HP-500 (TFA) insert). The vessel volume is 80 mL, which can bear max pressure 350 psi, and max temperature 210 °C to have the maximum safety during operation of irradiation. Pye Unicam SP300 spectrometer is used to record the IR spectra. All samples were measured using potassium bromide disks (KBr). The 1H NMR spectra for all samples were recorded on 500 MHz Bruker spectrometer and the chemical shifts δ downfield from tetramethyl silane (TMS) as an internal standard. The Shimadzu 3600 UV-VIS-NIR spectrophotometer was used to record the UV-visible spectra for the novel Schiff's bases. The required starting thiazole derivatives 2-aminothiazole **2a** and 2-amino-5-methyl-4-phenyl thiazole **2c** were purchased from Aldrich and used as received mean, while 2-amino-4-phenylthiazole **2b** was prepared via several methodologies according to published methods (Alenzi et al., 2020).

2.1.2. Organic preparations

Synthesis of thiazole-based Schiff's bases **3a-c**.

Thermal method.

General procedure: 2,4-dihydroxy benzaldehyde (**1**) was condensed with the appropriate 2-aminothiazole derivatives **2a-c** in refluxing ethanol and using a catalytic amount of glacial acetic acid. Condensation of all reactants was performed thermally for 8 h. The condensation reaction progressed smoothly to give the corresponding Schiff's base products in moderate to good yields. Recrystallization of the synthesized Schiff's bases **3a-c** was achieved using EtOH/DMF mixture solvent to give the corresponding thiazole-based Schiff's bases **3a-c**.

Microwave method.

General procedure: A mixture of 2,4-dihydroxy benzaldehyde (**1**) (10 mmol) and the suitable 2-aminothiazole derivatives **2a-c** (10 mmol) in ethanol (30 mL) was merged in a HP-500 process vessel. The vessel was capped tightly and irradiated using microwaves irradiation (600 W power) using pressurized conditions at 80 °C for a period 20 min. The reaction vessel was then left to cool then the resulting product was filtered, washed, and purified by recrystallization from EtOH/DMF mixture solvent to afford the titled compound **3a-c**. The physical constants of the products and their spectral data are given below:

4-((thiazol-2-ylimino)methyl)benzene-1,3-diol (**3a**).

Yield 70 %, mp. 278–279 °C, 1H NMR spectrum (500 MHz, $DMSO-d_6$), δ , ppm: 6.32 (s, 1H), 6.43–6.50 (m, 3H), 7.55 (m, 2H), 9.13 (s, 1H), 9.90–12.5 (s, 1H). IR spectrum (KBr disk, cm^{-1}), 3425 (O–H), 3040 (CH), 1630 (C = N). Anal. calcd. for $C_{10}H_8N_2O_2S$ (220.25): C, 54.53; H, 3.66; N, 12.72. Found: C, 54.51; H, 3.68; N, 12.68 %.

4-(((4-phenylthiazol-2-yl)imino)methyl)benzene-1,3-diol (**3b**).

Yield 60 %, mp. 237–238 °C, 1H NMR spectrum (500 MHz, $DMSO-d_6$), δ , ppm: 6.39 (s, 1H), 6.46(d, 1H), 7.32 (t, 1H), 7.42 (t, 2H), 7.66 (d, 1H), 7.89 (s, 1H), 7.95 (d, 2H), 9.20 (s, 1H), 11.50–12.5 (br, 2H, OH). IR spectrum (KBr disk, cm^{-1}), 3425 (O–H), 3040 (CH), 1630 (C = N). Anal. calcd. for $C_{16}H_{12}N_2O_2S$ (296.34): C, 64.85; H, 4.08; N, 9.45. Found: C, 64.83; H, 4.05; N, 9.40 %.

4-(((5-methyl-4-phenylthiazol-2-yl)imino)methyl)benzene-1,3-diol (**3c**).

Yield 64 %, mp. 243–244 °C, 1H NMR spectrum (500 MHz, $DMSO-d_6$), δ , ppm: 6.36 (s, 1H), 6.43 (d, 1H), 7.35 (t, 1H), 7.42 (t, 2H), 7.46 (m, 2H), 7.62 (m, 3H), 9.08 (s, 1H), 11.50–12.5 (br, 2H, OH). IR spectrum (KBr disk, cm^{-1}), 3425 (O–H), 3040 (CH), 1630 (C = N). Anal. calcd. for $C_{17}H_{14}N_2O_2S$ (310.37): C, 65.79; H, 4.55; N, 9.03. Found: C, 65.75; H, 4.52; N, 9.06 %.

2.2. Electrochemical measurements

The mild steel specimens have the following composition (by weight %): 0.07 % carbon, 0.29 % manganese, 0.07 % silicon, 0.012 % sulfur, 0.021 % phosphorus, and the rest iron, each with a surface area of 0.5 cm^2 , were used. A 0.5 M H_2SO_4 solution was prepared by diluting 98 %

AR grade H₂SO₄. Inhibitors were dissolved in the H₂SO₄ solution to create stock solutions, which were then diluted to the desired concentrations. Electrochemical tests were performed using a three-electrode setup, featuring a platinum counter electrode and a Hg/Hg₂SO₄/SO₄²⁻ reference electrode connected to a fine Luggin capillary. The working electrode's surface was polished, rinsed, degreased, and dried before the experiments. The open circuit potential (OCP) of the electrode was monitored for a duration of 30 min at a temperature of 25 °C or until reaching a stable state. A PGSTAT30 potentiostat/galvanostat was used for all measurements. Potentiodynamic polarization curves were obtained by sweeping the potential -150 mV to 150 mV relative to the OCP at a scan rate of 2 mV/s. Current densities were then determined using the apparent surface area of the electrode.

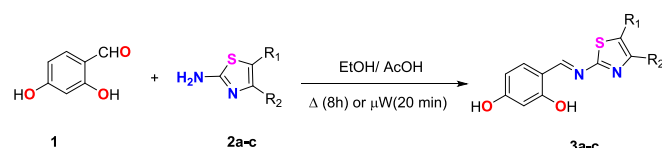
2.3. Computational methods

With the use of the Gaussian 09 software package (Becke, 1993; Stephens et al., 1994; Wysoglad et al., 2018), the geometric configuration was optimized using the density functional theory (DFT) B3LYP approach with the standard 6-31G(d,p) basis set. By combining the Lee-Yang-Parr correlation (BLYP) approach with a double zeta plus polarization (DNP) basis set and the generalized gradient approximation (GGA) functional of Becke exchange (Deng et al., 2014; Xu et al., 2015), geometric optimizations were accomplished with no symmetry constraints.

3. Results and discussion

3.1. Synthesis and structure elucidation of 3a-c

The targeted Schiff's bases were prepared by the reported procedure with some modifications. Thus, 2,4-dihydroxy benzaldehyde (1) was condensed with the appropriate 2-aminothiazole derivatives 2a-c in refluxing ethanol and using a catalytic amount of glacial acetic acid. Condensation of all reactants was performed either thermally for 8 h. or under microwave irradiation conditions as shown in Scheme 1. The microwave irradiation has been accomplished using a CEM microwave reactor station using pressurized conditions with power of 600 W for 20 min at the boiling point of the alcohol. Although there was no great improve in the yield of the product, but the time of the synthesis was reduced dramatically by using the microwaves irradiation. The reaction progressed smoothly to give the corresponding Schiff's base products in good yields. The structure of the isolated Schiff's bases 3a-c was confirmed using spectroscopic tools of analyses. For instance, ¹H NMR spectrum of Schiff's base 3b showed a singlet signal characteristic to the methine group proton (CH = N) at δ 9.20 ppm proton, a singlet signal characteristic to the thiazole ring proton at δ 7.89 ppm proton, a singlet signal characteristic to the aromatic ring proton of the aldehyde moiety at δ 6.39 ppm proton, the broad band characteristic to the hydroxyl groups resonate in the range between 11.5 and 12,5 and other aromatic



No.	R ₁	R ₂	Yield %	
			Thermal Method	Microwave Method
2a	H	H	65	70
2b	H	Ph	58	60
2c	CH ₃	Ph	62	64

Scheme 1. Synthesis of Schiff's based 3a-c under thermal and microwave irradiation conditions.

ring protons in the range of δ 6.46–6.98 ppm as showed in the ¹H NMR spectrum of 3b in Fig. 1. The IR spectrum of the 3a-c derivative showed the main characteristic bands at 3046 and 1630 assigned to CH aromatic stretching and C = N group vibration, respectively (Fig. 2).

The electronic spectra of all the thiazole Schiff bases 3a-c were recorded in the methanol (MeOH) solvent at ambient temperature in the wavelength region of 200–1000 nm. As seen in Fig. 3, the electronic spectra of the synthesized Schiff bases 3a-c revealed two absorption bands, in which the first band appear at 279–314 nm are attributable to an apparent π → π* transition inside the aromatic ring (Affat, 2022), as well 3a-c exhibited a second broad band at 381, 383 and 385 nm, respectively. In compounds 3a-c, the recorded band identified at 381–385 nm was ascribed to the CH = N (azomethine) unit with n → π* electronic interactions of conjugation between the electrons lone pair and the conjugated double bond of the aromatic ring. (Affat, 2022).

3.2. Application of Schiff bases 3a-c as corrosion inhibitors: Evaluation by electrochemical measurements

Numerous Schiff-base inhibitors have been developed for use in aqueous media, demonstrating effectiveness across a wide range of metals and alloys. These inhibitors are particularly efficient due to the presence of an azomethine group (-CHN-) in their molecular structure. Beyond the imine group, the substitution of other components also plays a crucial role in determining inhibitory activity. Some Schiff base compounds have been found to exhibit significantly greater inhibition activity compared to analogous amine and carbonyl compounds. This study aims to investigate the corrosion inhibition effectiveness of newly synthesized Schiff base compounds 3a-c on carbon steel. This investigation will compare the corrosion behavior of carbon steel both in the absence and presence of these compounds using electrochemical measurements. Fig. 4 depicts the potentiodynamic polarization curves obtained for mild steel in 0.5 M H₂SO₄ under two conditions: (a) without any inhibitor and in the presence of inhibitors (b) 3b, (c) 3a, and (d) 3c at 25 °C. The data extracted from this figure are summarized in Table 1.

The efficiency of the inhibitors (P_{icorr}) was calculated using the following equation:

$$P_{icorr} = 100 \times \frac{(i_{corr}(\text{uninhibited}) - i_{corr}(\text{inhibited}))}{i_{corr}(\text{uninhibited})} \quad (1)$$

The corrosion current in the absence and presence of inhibitor is denoted as *i*_{corr}(uninhibited) and *i*_{corr}(inhibited), respectively. P_{icorr} was found to be in the order of 3c > 3b > 3a. In the presence of 0.5 mM inhibitor, the P_{icorr} values were 48 %, 69 %, and 75 % for 3a, 3b, and 3c, respectively. This trend can be attributed to the electron density on the heterocyclic 5 ring "Thiazole". In 3a, the ring is unsubstituted, while in 3b, it is substituted by a phenyl ring, which could enhance adsorption. In 3c, the heterocyclic ring is substituted by a methyl group, further increasing the electron-donating ability of the inhibitor. The corrosion potential shifts were not significant.

The inhibition efficiency (IE) calculated based on the polarization resistance (R_p) can be expressed as:

$$P_{Rp} = \frac{R_p(\text{inhibitor}) - R_p(\text{without inhibitor})}{R_p(\text{inhibitor})} \times 100 \quad (2)$$

where: R_p(without inhibitor) is the polarization resistance of the uninhibited system, and R_p(inhibitor) is the polarization resistance of the inhibited system. As shown in Table 1, there is a high consistency between the inhibition efficiencies calculated based on the corrosion current and those calculated based on the polarization resistance.

As shown in Table 1, the impact of inhibitor concentration on the Tafel slopes was minimal, suggesting that the inhibitor most likely functions by simply blocking the surface without altering the underlying mechanism. The interactions of Schiff base with metallic surfaces can be further elucidated using quantum chemistry calculations (Ebenso et al.,

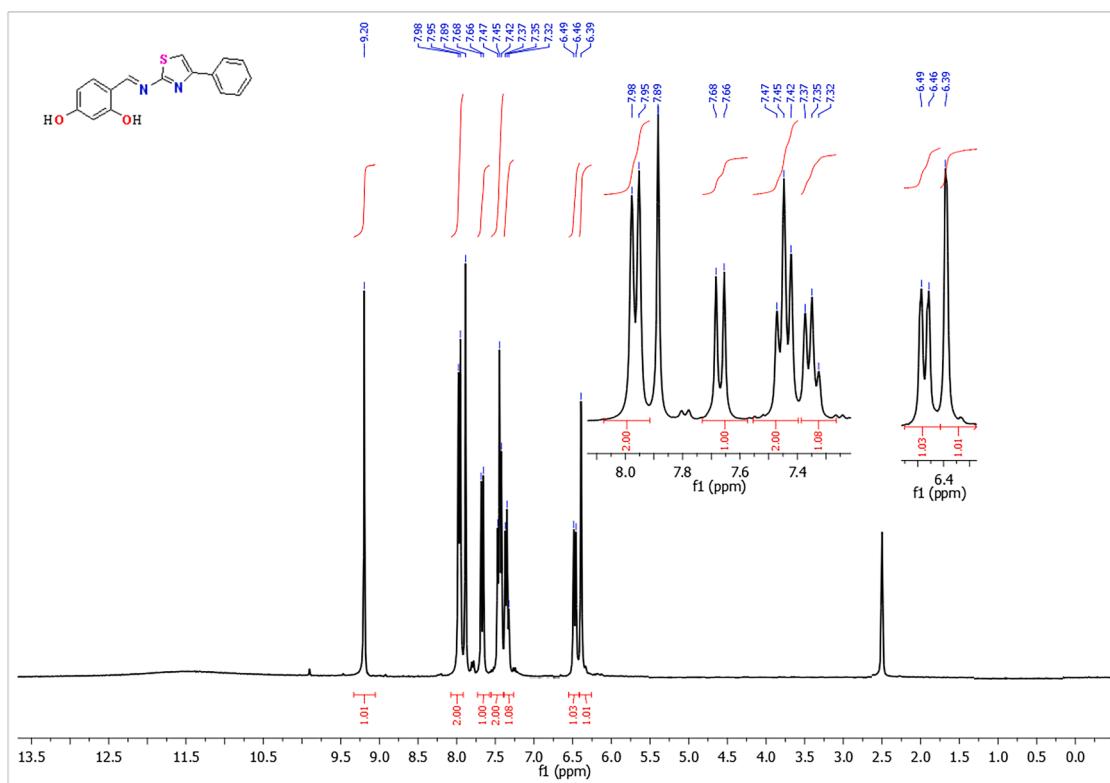


Fig. 1. The ¹H NMR spectrum of Schiff's base 3b.

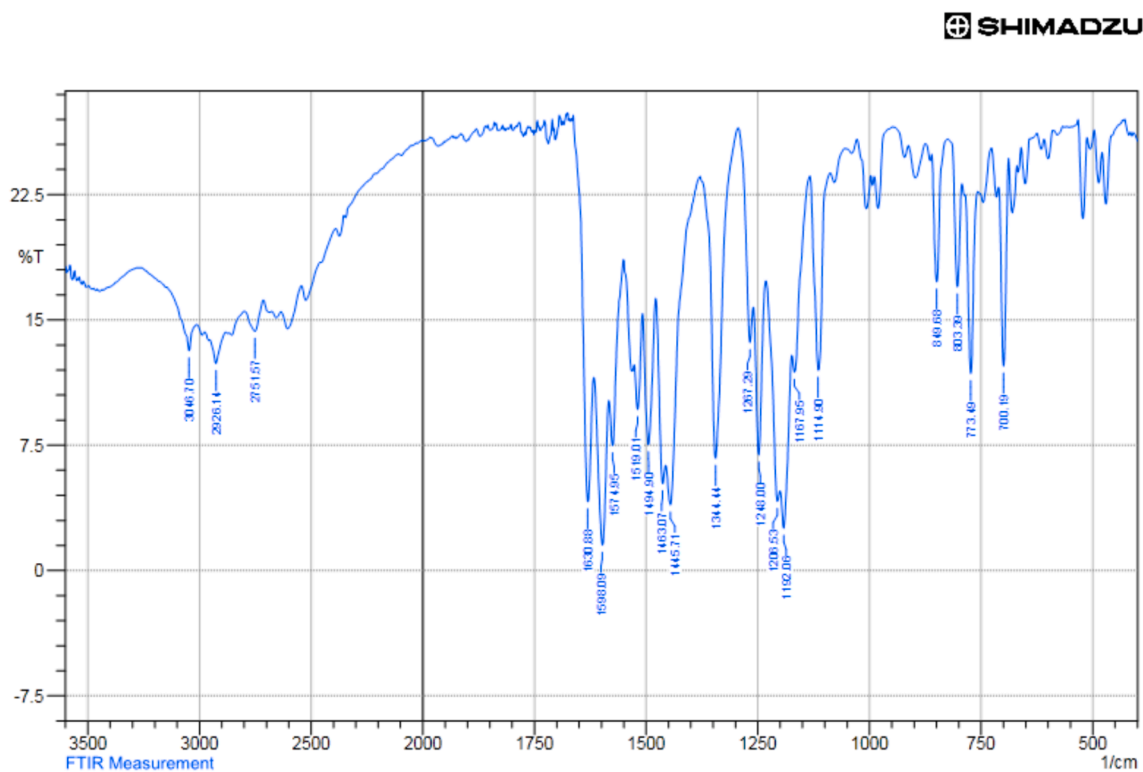


Fig. 2. The IR spectrum of Schiff's base 3b.

2021).

The insignificant effect of inhibitor concentration on the Tafel slopes suggests that the inhibitor acts through a simple blocking mechanism,

with its adsorption not altering the reaction mechanism (Cao, 1996).

The experimental data were fitted to various isotherms including Langmuir, Temkin, and Flory–Huggins isotherms, and was found accord

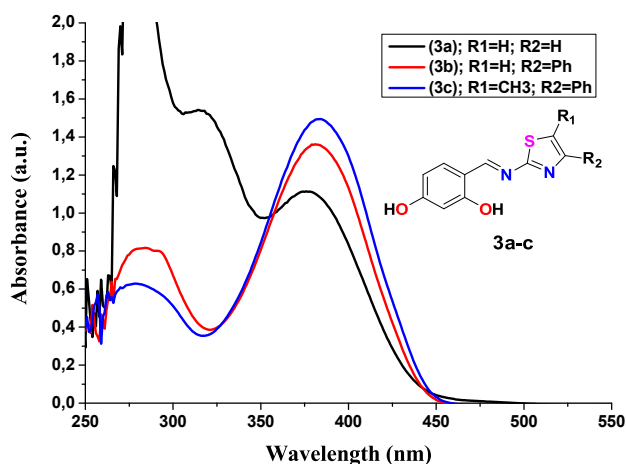


Fig. 3. Absorption spectra of thiazole-based Schiff-base **3a-c** (30 mM) recorded in MeOH solvent.

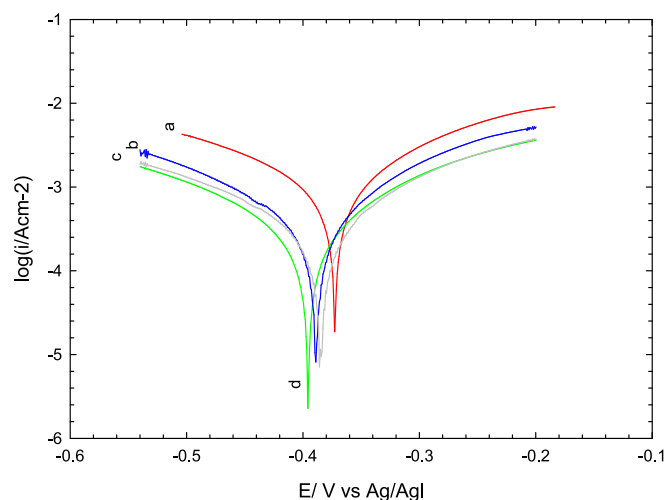


Fig. 4. potentiodynamic polarization curves obtained for mild steel in 0.5 M H_2SO_4 under two conditions: (a) in the absence of inhibitors and in the presence of 0.5 mM of inhibitors (b) **3a**, (c) **3b**, and (d) **3c** at 25 °C.

Table 1

corrosion current, corrosion potential, protection efficiency and surface coverage obtained in the presence of 0.5 mM Inhibitors. Data were extracted from Fig. 4.

	$I_{corr} / A \times 10^4$	$-E_{corr} / mV$	β_a	β_c	$P_{i_{corr}}$	R_p / Ω	P_{Rp}	θ
Blank	12.8	388	119	131	—	26	—	—
3a	6.65	390	114	122	48	55	52	0.48
3b	3.16	395	114	121	69	83	68	0.69
3c	3.2	377	121	109	75	96	73	0.75

with Temkin isotherm (Eq. (2) (Bilgic and Cahskan, 1999; Priya et al., 2008) and the plots are presented in Fig. 5.

$$\text{Exp}(-2a\theta) = KC \quad (3)$$

here, θ represents the surface coverage degree (derived from the previously illustrated polarization curves), C stands for the inhibitor con-

centration, a (J/mol) denotes the molecular interaction parameter, It offers insights into the interactions occurring within the adsorbed layer. and K (mol/L) represents the equilibrium constant of the adsorption process.

The equilibrium constant of the adsorption process can be linked to the standard free energy of adsorption using the following equation (Li et al., 2008; Cano et al., 2004):

$$\Delta G_{ads} = -RT \ln(55.5K) \quad (4)$$

The value 55.5 represents the concentration of water expressed in mol dm^{-3} . The adsorption parameters obtained from the plots are detailed in Table 2. This table shows that the values of the free energy of adsorption (ΔG_{ads}) are negative, ranging from -33.97 to $-40.76 \text{ kJ mol}^{-1}$ for **3a** and **3c**, respectively.

The negative values of ΔG_{ads} indicate a spontaneous adsorption process. The range of ΔG_{ads} values obtained in this study (-33.97 to $-40.7 \text{ kJ mol}^{-1}$) implies that the inhibitor's adsorption involves both physisorption and chemisorption. Hence, the adsorption of molecules on the mild steel surface from a 0.5 M H_2SO_4 solution is attributed to a concurrent physical and chemical process.

3.3. Quantum chemical calculations (DFT)

To develop novel and potent inhibitors, calculations based on density functional theory (DFT) are frequently utilized to investigate and assess the various reactivity parameters and find the relationship between the empirically measured inhibitory efficiency and theoretically obtained parameters (Geerlings et al., 2003; Kokalj, 2021; Gece, 2008; Obot et al., 2015; Lemilemu et al., 2021). In this context, we analyzed quantum mechanical descriptors for the three synthesized thiazole-based Schiff base molecules **3a-c**. The results are shown in Table 3. The molecules' wave function distribution and relative reactivity were examined using the HOMO and LUMO frontier molecular orbitals (Fig. 6). In addition, the mechanism of a molecule's adsorption onto a metallic surface has been demonstrated to be significantly influenced by HOMO and LUMO frontier molecular orbitals, as well associated to the molecule's susceptibility to electrophile and nucleophile attack. It is established that an inhibitor with a higher HOMO value has a greater ability to share electrons. However, the likelihood that the molecule will accept electrons is indicated by lower LUMO values (Gece, 2008). The energy gaps (in eV) were calculated to be 3.633, 3.416 and 3.454 for compounds **3a**, **3b** and **3c**, respectively (Table 3). According to the results, the synthesized compounds exhibit good reactivity. The findings also showed that substituted thiazole-derived Schiff bases **3b** and **3c** has the lowest HOMO–LUMO energy gap compared to their unsubstituted thiazole analogue **3a**, which indicates that it has a significant intramolecular charge transfer, high chemical reactivity and better inhibition efficiency. Furthermore, compound **3c** showed large HOMO value -5.500 eV . It is therefore reasonable to conclude that **3c** would demonstrate a better affinity for the adsorption onto the MS surface via the unoccupied iron d-orbital through the lone pair electrons on the N and O atoms.

Chemical (σ) softness parameter has also been found to represent another useful quantity that provides information on the interaction of molecules with a metallic surface, in which metals are regarded as soft acids while inhibitor compounds as soft bases according to the HASB principle (Obot and Gasem, 2014). Inhibitors with higher chemical (σ) softness are more easily adsorbed on metallic surfaces. The results further revealed that compound **3c** has greater chemical (σ) compared to **3a** signifying better adsorptive tendency for the Fe surface (Deng et al., 2014; Yadav et al., 2016).

Moreover, the electro-donating and electro-accepting powers, ω^+ and

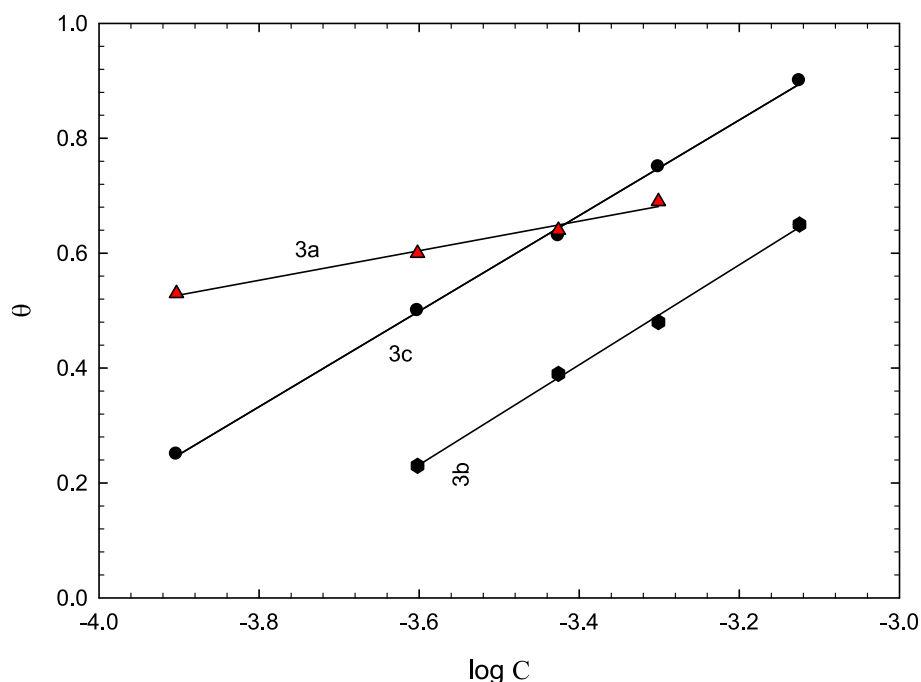


Fig. 5. Temkin adsorption isotherm for 3a, 3b and 3c.

Table 2

Calculated values obtained from Temkin isotherm for 3a and 3c.

Inhibitor	A"/J/mol"	K(mol/L)	R ²	G°/ kJ/mol
3a	-4.4	7.3 × 10 ⁴	0.99	- 33.97
3b	-1.32	7.2 × 10 ³	0.99	-30.56
3c	-1.38	1.5 × 10 ⁴	0.99	- 40.7

ω^+ , have been proposed as a new reactivity index and defined by Gázquez et al. (Gázquez et al., 2007; Domingo and Pérez, 2011) as,

$$\omega^- = \frac{(A + 3I)^2}{16 \times (I - A)} \quad (5)$$

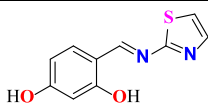
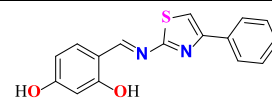
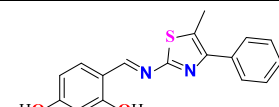
$$\omega^+ = \frac{(I + 3A)^2}{16 \times (I - A)} \quad (6)$$

where ω^- and ω^+ denotes, respectively, the measure of a system's tendency to donate and accept charge. It is important to note that a higher value of ω^+ indicates a system with a superior ability to accept charges, whereas a lower value of ω^+ indicates an electron donor character that is more favorable. Table 3 lists and collects both ω^+ and ω^- quantities. According to Table 3, molecule 3c has the highest capacity to donate charge, with $\omega^+ = 2.451$ eV.

On the other hand, the equation (6) can be used to calculate the fraction of electrons transferred (ΔN) from an anticorrosive molecule to a metallic atom (Chauhan and Gunasekaran, 2007; Wahyuningrum et al., 2008; Benmessaoud et al., 2007; Rodríguez-Valdez et al., 2006).

Table 3

Calculated theoretical chemical parameters for anticorrosive Schiff bases molecules 3a-c.

Descriptors			
	3a	3b	3c
HOMO	-5.757 (eV)	-5.570 (eV)	-5.500 (eV)
LUMO	-2.124 (eV)	-2.154 (eV)	-2.046 (eV)
$\Delta E(\text{HOMO-LUMO})$	3.633 (eV)	3.416 (eV)	3.454 (eV)
Ionization energy (I)	5.757 (eV)	5.570 (eV)	5.500 (eV)
Electron affinity (A)	2.124 (eV)	2.154 (eV)	2.046 (eV)
Dipole moment (Debye)	1.989	1.917	1.803
$\eta = E_L - E_H$	3.633 (eV)	3.416 (eV)	3.454 (eV)
$\mu = (E_H + E_L)/2$	-3.940 (eV)	-3.862 (eV)	-3.773 (eV)
Global softness (σ)	0.275	0.293	0.289
Electronegativity (χ)	3.940 (eV)	3.862 (eV)	3.773 (eV)
$\omega = (-\mu^2/2\eta)$	2.136 (eV)	2.183 (eV)	2.061 (eV)
Electroaccepting (ω^+) power	2.531	2.649	2.451
Electrodonating (ω^-) power	6.471	6.511	6.224
Net electrophilicity ($\Delta\omega^\pm$)	9.002	9.160	8.675
ΔN	1.084	1.131	1.092
Fraction of transferred electrons (ΔN)	0.421	0.459	0.467
ΔE back-donation	-0.908	-0.854	-0.863

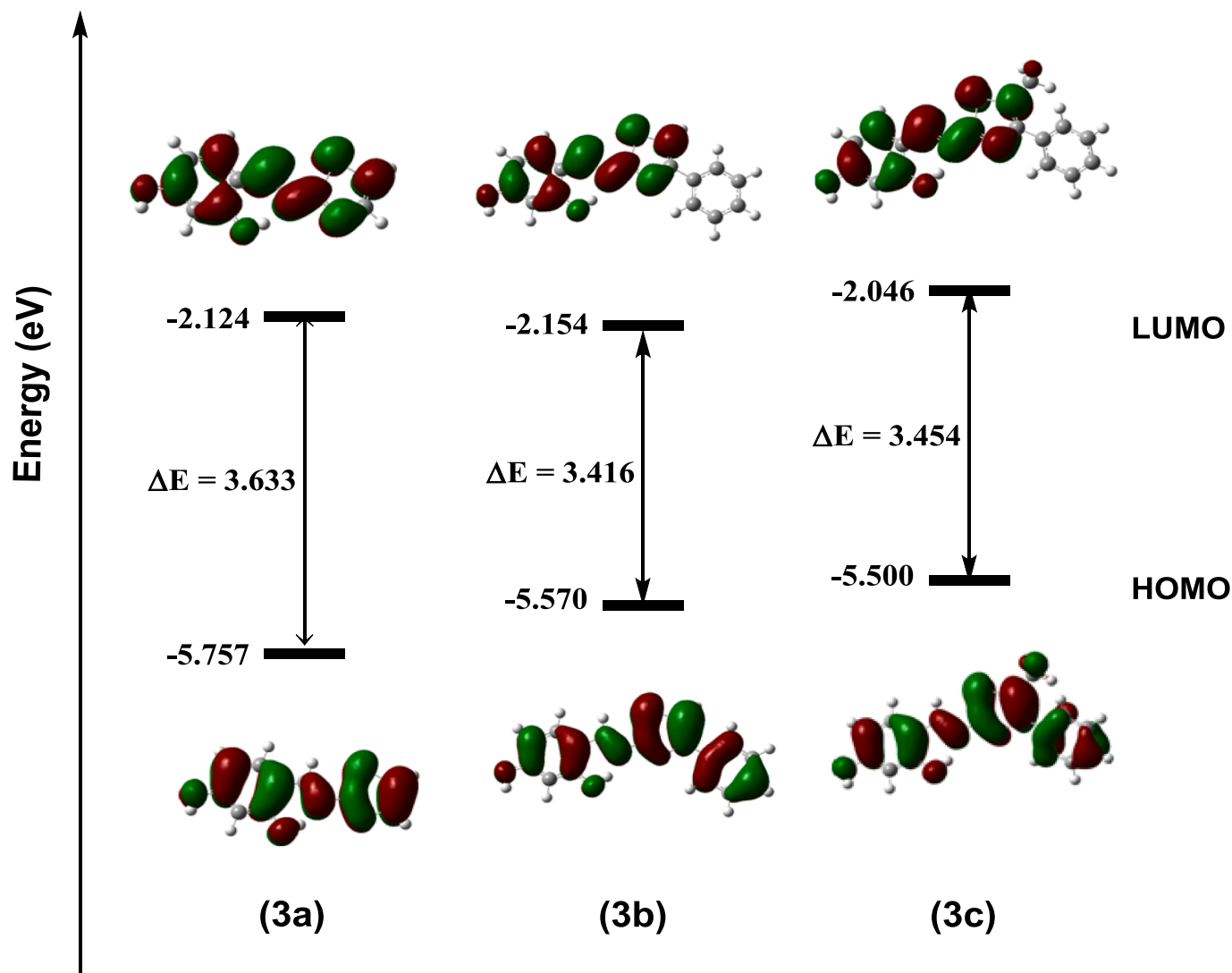


Fig. 6. Optimized structure, HOMO, LUMO surfaces for anticorrosive Schiff bases molecules (3a-c).

$$\Delta N = \frac{\chi_{Fe} - \chi_{inh}}{2 \times (\eta_{Fe} + \eta_{inh})} \quad (7)$$

where χ_{inh} and η_{inh} , χ_{Fe} and η_{Fe} and denotes the absolute electronegativity and hardness of anticorrosive molecule and iron atom, respectively. The values of $\eta_{Fe} = 0$ and $\chi_{Fe} = 7$ eV have been reported theoretically (Chauhan and Gunasekaran, 2007; Wahyuningrum et al., 2008; Benmessaoud et al., 2007; Rodríguez-Valdez et al., 2006), related to the metallic neutral atoms' properties.

Table 3 displays the theoretical values of the transferred fractions. It has been found that a high anticorrosive efficiency is correlated with a large value of ΔN . Our findings also support the earlier behavior, as the higher value of ΔN corresponds to a molecule 3c, whose $\Delta N = 0.467$ indicates a more effective anticorrosive behavior.

Moreover, the anticorrosive molecule-metallic surface interaction has been evaluated (Gómez et al., 2006) by the electronic back-donation concept, defined as $\Delta E_{Back-donation} = -\eta/4$, in which if $\eta > 0$ that implies $\Delta E_{Back-donation} < 0$, and indicates that back-donation process from the anticorrosive molecule to metal is energetically favored. As shown in

Table 3 the value of $\Delta E_{Back-donation}$ for our anticorrosive thiazole-based Schiff base molecules 3a-c are negative, indicating that the charge transfer is energetically favorable. This enables us to compare anticorrosive efficiency of molecules, in which an increase in stabilization energy arising from the interaction between the anticorrosive molecule and the metallic surface should lead to an increase in anticorrosive efficiency. In line with the experimental findings, the calculated $\Delta E_{Back-donation}$ values show the following tendency: (3c) > (3a).

Mulliken charges.

In order to estimate the inhibitors' adsorption center and characterize possible interactions between the molecules and the Fe surface, the Mulliken charges for the Schiff bases molecules (3a-c) are computed and shown in Fig. 7. It is noteworthy that the highest negative charge atoms have a strong tendency on the metallic surface. However, it is obvious that the inhibitor molecules can interact through a variety of active centers (N, O) with the metallic surface. The results showed that in (3a-c) compounds, the O atom has a greater excess of negative charge. This implies that by adsorbing to the C-steel's surface through its active sites, the studied Schiff-bases employed as inhibitors can effectively

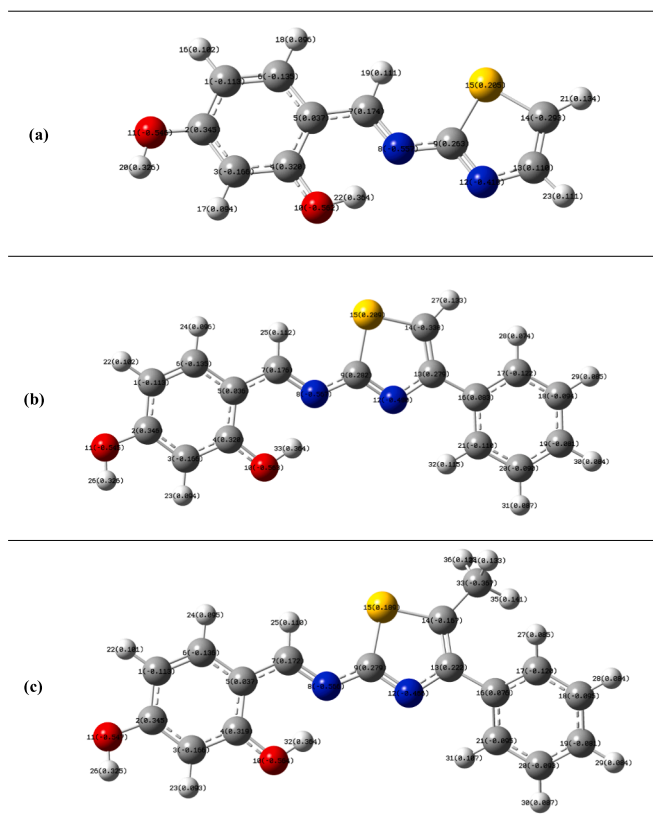


Fig. 7. Mulliken charges for the anticorrosive Schiff bases molecules (3a-c).

prevent corrosion of the metal. Furthermore, since the sulfur atoms in Schiff base molecules have an excess of positive charge and are able to accept electrons from orbital 3d of the iron atoms (Fe) to generate a feedback bond, it is evident that the sulfur atoms act mostly as electrophilic centers. Thus, in order to improve the interaction between the inhibitor and metallic surface, it seems that this process is necessary to maintain equilibrium and prevent the accumulation of negative charges on the metal surface. It is also important to note that a good corrosion inhibitor with high inhibition efficiency can accept free electrons from the metal in addition to offering electrons to vacant orbitals. Accordingly, it should be noted that the molecular electronic parameters and the quantum chemical calculation method discussed above could be an important factor in providing us with a broad overview of the inhibitor molecule's mode of action and contributing to the assessment of inhibition efficiency.

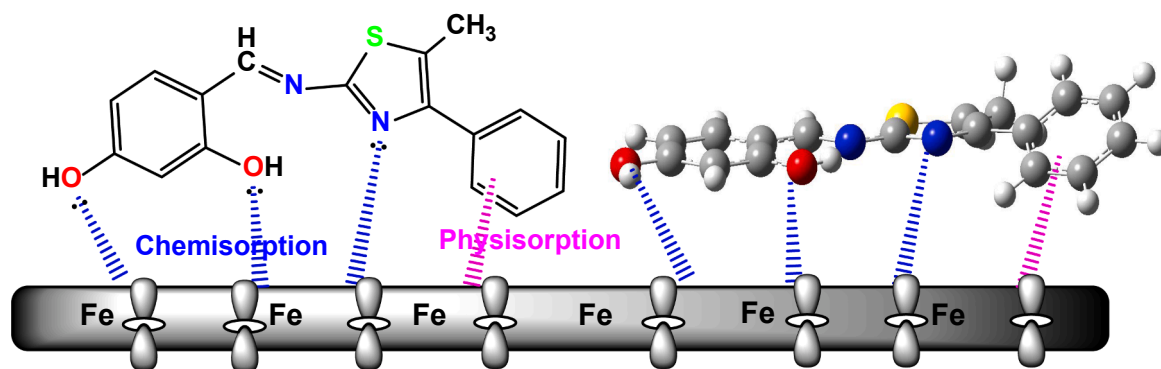


Fig. 8. Adsorption mechanism of Schiff bases molecule 3c on carbon steel surface in 0.5 M H_2SO_4 .

Mechanism of inhibition

A number of factors, such as the inhibitor molecules' atomic charges and chemical structure, as well as behavior in an acidic environment, influence the inhibitor molecules' adsorption onto the metallic surface. The assumptions made by the Temkin adsorption model on how the Schiff bases molecules (3a-c) adsorb to the metallic substrate were also validated by the adsorption isotherm explorations. Electron pairs of heteroatoms in the Schiff bases molecules (3a-c) facilitate chemical adsorption onto the metallic substrate. The suggested mechanism for protecting metallic substrates against corrosion in an acidic media is shown in Fig. 8. As demonstrated in Fig. 8, the thiazole-based Schiff base derivatives exhibited good corrosion inhibition properties due to their affinity to be adsorbed on the surface of carbon steel alloy by mutual chemisorption and physisorption. Chemisorption occurs when coordinating bonds are formed between the lone pairs in thiazole-based Schiff base derivatives and the surface of the carbon steel alloy containing empty Fe atom d-orbitals. Consequently, through a combination of physical and chemical interactions, the Schiff bases molecules can form a strong adhesive adsorbed layer on the surface of the CS alloy, protecting it from further dissolution by isolating the surface from an aggressive environment.

4. Conclusion

In this study, three novel thiazole-based Schiff's base derivatives were synthesized using thermal as well as microwave irradiation. The novel Schiff's bases were investigated using analytical, spectroscopic, and physical methods. The synthesized compounds demonstrated efficacy as corrosion inhibitors for mild steel pipelines in H_2SO_4 solution. Their corrosion inhibition mechanism involves adsorption according to the Temkin model, with the mode of adsorption identified as mixed type based on the values of free energy change. This suggests that physico-chemical adsorption governs the distribution of these organic inhibitors on the CS alloy surface in the aggressive acidic medium. Quantum chemical calculations based on DFT studies were effectively utilized at the B3LYP level of theory to provide optimal molecular structures with electronic calculations. The calculated global hardness values were lower than the predicted global softness values, suggesting that the thiazole-based Schiff base under investigation were less stable and more reactive. The obtained results clearly show that the presence of both an electron-rich and a π -electron moiety should influence the electronic structure of an inhibitor molecule and facilitate its ability to readily remove water molecules from the metal surface. All the experimental results were consistency with the theoretical DFT calculations, which provided a clear explanation of the relationship between inhibitor molecular structures and inhibition efficiency.

CRediT authorship contribution statement

Nizar El Guesmi: Conceptualization, Data curation, Methodology, Writing – original draft, Writing – review & editing. **Basim H. Asghar:** Data curation, Investigation, Methodology, Project administration, Writing – review & editing. **Mohamed I. Awad:** Data curation, Investigation, Methodology, Writing – original draft, Writing – review & editing. **Abdulrahman N. Al Harbi:** Data curation, Methodology, Software, Visualization, Writing – original draft. **Mohammed A. Kassem:** Data curation, Methodology, Visualization, Writing – review & editing. **Mohamed R. Shaaban:** Data curation, Investigation, Methodology, Supervision, Validation, Writing – original draft, Writing – review & editing.

Declaration of Competing Interest

The authors declare that they have no known competing financial interests or personal relationships that could have appeared to influence the work reported in this paper.

Appendix A. Supplementary data

Supplementary data to this article can be found online at <https://doi.org/10.1016/j.arabjc.2024.105867>.

References

- Abdalla, T.H., Nasr, A.S., Bassioni, G., Harding, D.R., Kandile, N.G., 2022. Fabrication of sustainable hydrogels-based chitosan Schiff base and their potential applications. *Arabian Journal of Chemistry*. 15, 103511.
- Abdallah, M., Al Bahir, A., Altass, H.M., Fawzy, A., El Guesmi, N., Al-Gorair, A.S., Benhiba, F., Warad, I., Zarrouk, A., 2021a. Anticorrosion and adsorption performance of expired antibacterial drugs on Sabc iron corrosion in HCl solution: Chemical, electrochemical and theoretical approach. *Journal of Molecular Liquids*. 330, 115702.
- Abdallah, M., El Guesmi, N., Al-Gorair, A.S., El-Sayed, R., Meshabi, A., Sobhi, M., 2021b. Enhancing the anticorrosion performance of mild steel in sulfuric acid using synthetic non-ionic surfactants: practical and theoretical studies. *Green Chemistry Letters and Reviews*. 14, 381–393.
- Abdel-karim, A.M., Hussien, H.M., Shahen, S., El-Shamy, O.A.A., Ghayad, I.M., Saleh, N. M., Abd El-Sattar, N.E.A., 2024. Green synthesis of novel bis structure of (Carbamothioyl) oxalamide derivatives as corrosion inhibitors for copper in 3.5% NaCl; experimental and theoretical investigation. *Journal of Molecular Structure*, 1295, 136597.
- Abd-elmaksoud, G.A., Abusaif, M.S., Ammar, Y.A., Al-Sharbasy, S., Migahed, M.A., 2023. Construction, Characterization, DFT Computational Study, and Evaluation of the Performance of Some New N-Amino Pyridinone Schiff Base Catalyzed with Cerium(IV) Ammonium Nitrate (CAN) as Corrosion Inhibitors in Some Petroleum Applications. *Arab J Sci Eng*. 48, 16167–16185.
- Abdelsalam, M.M., Bedair, M.A., Hassan, A.M., Heakal, B.H., Younis, A., Elbially, Z.I., Badawy, M.A., El-Din Fawzy, H., Fareed, S.A., 2022. Green synthesis, electrochemical, and DFT studies on the corrosion inhibition of steel by some novel triazole Schiff base derivatives in hydrochloric acid solution. *Arabian Journal of Chemistry*. 15, 103491.
- Affat, S.S., 2022. Experimental and Theoretical Studies of New Schiff Base as a Corrosion Inhibitor in Acidic Media and Study Antioxidant Activity. *Iran. J. Chem. Chem. Eng.* 41, 3351–3364.
- Ahmed, M., Qadir, M.A., Shafiq, M.I., Muddassar, M., Samra, Z.Q., Hameed, A., 2019. Synthesis, characterization, biological activities and molecular modeling of Schiff bases of benzene sulfonamides bearing curcumin scaffold. *Arabian Journal of Chemistry*. 12, 41–53.
- Al-Amiery, A.A., Al-Azzawi, W.K., Wan Isahak, W.N.R., 2022. Isatin Schiff base is an effective corrosion inhibitor for mild steel in hydrochloric acid solution: gravimetric, electrochemical, and computational investigation. *Scientific Reports*. 12, 17773.
- Alenzi, R.A., El Guesmi, N., Shaaban, M.R., Asghar, B.H., Farghaly, T.A., 2020. Assessing the nucleophilic character of 2-amino-4-arylthiazoles through coupling with 4,6-dinitrobenzofuroxan: Experimental and theoretical approaches based on structure-reactivity relationships. *Journal of Saudi Chemical Society*. 24, 754–764.
- Alorini, T.A., Al-Hakimi, A.N., El-Sayed Saeed, S., Alhamzi, L., E. H., Albadri, A. E.A.E., 2022. Synthesis, characterization, and anticancer activity of some metal complexes with a new Schiff base ligand. *Arabian Journal of Chemistry*. 15, 103559.
- Altalhi, A.A., 2023. Anticorrosion Investigation of New Diazene-Based Schiff Base Derivatives as Safe Corrosion Inhibitors for API X65 Steel Pipelines in Acidic Oilfield Formation Water: Synthesis, Experimental, and Computational Studies. *ACS Omega*. 8, 31271–31280.
- Alzaharani, L., El-Ghamry, H.A., Saber, A.L., Mohammed, G.I., 2023. Spectrophotometric determination of Mercury(II) ions in laboratory and Zamzam water using bis Schiff base ligand based on 1,2,4-Triazole-3,5-diamine and o-Vaniline. *Arabian Journal of Chemistry*. 16, 104418.
- Arslan, T., Kandemirli, F., Ebenso, E.E., Love, I., Alemu, H., 2009. Quantum chemical studies on the corrosion inhibition of some sulphonamides on mild steel in acidic medium. *Corros. Sci.* 51, 35–47.
- Becke, A.D., 1993. Density-functional thermochemistry. III. The role of exact exchange. *J. Chem. Phys.* 98, 5648–5652.
- Benmessoud, M., Es-Salah, K., Hajjaji, N., Takenouti, H., Shri, A., Ebentouhami, M., 2007. Inhibiting effect of 2-mercaptobenzimidazole on the corrosion of Cu–30Ni alloy in aerated 3% NaCl in presence of ammonia. *Corros. Sci.* 49, 3880–3888.
- Berhanu, A.L., Mohiuddin, I., Malik, A.K., Aulakh, J.S., Kumar, V., Kim, K.-H., 2019. A review of the applications of Schiff bases as optical chemical sensors. *TRAC Trends Anal. Chem.* 116, 74–91.
- Betti, N., Al-Amiery, A.A., Al-Azzawi, W.K., Wan Isahak, W.N.R., 2023. Corrosion inhibition properties of schiff base derivative against mild steel in HCl environment complemented with DFT investigations. *Scientific Reports*. 13, 8979.
- Bilgic, S., Calskan, N., 1999. The effect of N-(1-toluidine) salicylaldehyde on the corrosion of austenitic chromium–nickel steel. *Appl. Surf. Sci.* 152, 107–114.
- Cano, E., Polo, J.L., La Iglesia, A., Bastidas, J.M., 2004. A study on the adsorption of benzotriazole on copper in hydrochloric acid using the inflection point of the isotherm. *Adsorption*. 10, 219–225.
- Cao, C., 1996. On electrochemical techniques for interface inhibitor research. *Corros. Sci.* 38, 2073–2082.
- Chauhan, L.R., Gunasekaran, G., 2007. Corrosion inhibition of mild steel by plant extract in dilute HCl medium. *Corros. Sci.* 49, 1143–1161.
- Chugh, B., Singh, A.K., Thakur, S., Pani, B., Lgaz, H., Chung, I.-M., Jha, R., Ebenso, E.E., 2020. Comparative Investigation of Corrosion-Mitigating Behavior ofThiadiazole-Derived Bis-SchiffBases for Mild Steel in Acid Medium:Experimental, Theoretical, and Surface Study. *ACS Omega*. 5, 13503–13520.
- Deng, S.D., Li, X.H., Xie, X.G., 2014. Hydroxymethylurea and 1,3-bis(hydroxymethyl) urea as corrosion inhibitors for steel in HCl solution. *Corros. Sci.* 80, 276–289.
- Domingo, L.R., Pérez, P., 2011. The nucleophilicity N index in organic chemistry. *Org. Biomol. Chem.* 9, 7168–7175.
- Ebenso, E.E., Verma, C., Olasunkanmi, L.O., Akpan, E.D., Verma, D.K., Lgaz, H., Guo, L., Kaya, S., Quraishi, M.A., 2021. Molecular modelling of compounds used for corrosion inhibition studies: A review. *Phys. Chem. Chem. Phys.* 23, 19987–20027.
- El Guesmi, N., Ahmed, S.A., Maurel, F., Althagafi, I.I., Khairou, K.S., 2017. Photochromism of dihydroindolizines. Part XXII: Significant effect of region B substituents on tuning the photophysical properties of photochromic dihydroindolizines: Absorption, kinetic and computational studies. *J. Photochem. Photobiol. a. Chem.* 348, 125–133.
- El Guesmi, N., Hussein, E.M., Ahmed, S.A., 2019. MCM-SO3H catalyzed synthesis of environment-sensitive fluorophores incorporating pyrene moiety: Optimization, fluorescence emission and theoretical studies. *J. Photochem. Photobiol. a. Chem.* 371, 306–314.
- Fouda, A.S., Khalil, E.M., EL-Mahdy, G.A., Shaban, M.M., Mohammed, A.S., Abdelsatar, N.A., 2023. Synthesis and characterization of novel acrylamide derivatives and their use as corrosion inhibitors for carbon steel in hydrochloric acid solution. *Scientific Reports*. 13, 3519.
- Gázquez, J.L., Cedillo, A., Vela, A., 2007. Electrodonating and Electroaccepting Powers. *J. Phys. Chem. a*. 111, 1966–1970.
- Gece, G., 2008. The use of quantum chemical methods in corrosion inhibitor studies. *Corros. Sci.* 50, 2981–2992.
- Geerlings, P., De Proft, F., Langenaeker, W., 2003. Conceptual Density Functional Theory. *Chem. Rev.* 103, 1793–1874.
- Gómez, B., Likhanova, N.V., Domínguez-Aguilar, M.A., Martínez-Palou, R., Vela, A., Gázquez, J.L., 2006. Quantum Chemical Study of the Inhibitive Properties of 2-Pyridyl-Azoles. *J. Phys. Chem. b*. 110, 8928–8934.
- Gong, W., Yin, X., Liu, Y., Chen, Y., Yang, W., 2019. 2-Amino-4-(4-methoxyphenyl)thiazole as a novel corrosion inhibitor for mild steel in acidic medium. *Progress in Organic Coatings*. 126, 150–161.
- Guo, Y., Xu, B., Liu, Y., Yang, W., Yin, X., Chen, Y., Le, J., Chen, Z., 2017. Corrosion inhibition properties of two imidazolium ionic liquids with hydrophilic tetrafluoroborate and hydrophobic hexafluorophosphate anions in acid medium. *J. Ind. Eng. Chem.* 56, 234–247.
- Hamani, H., Douadi, T., Al-Noaimi, M., Issaadi, S., Daoud, D., Chafaa, S., 2014. Electrochemical and Quantum Chemical Studies of Some Azomethine Compounds as Corrosion Inhibitors for Mild Steel in 1M Hydrochloric Acid. *Corros. Sci.* 88, 234–245.
- Hegazy, M.A., Badawi, A.M., Abd El Rehim, S.S., Kamel, W.M., 2013. Corrosion inhibition of carbon steel using novel N-(2-(2-mercaptoacetoxy)ethyl)-N, N-dimethyl) dodecan-1-aminium bromide during acid pickling. *Corros. Sci.* 69, 110–122.
- Hussein, E.M., El Guesmi, N., Moussa, Z., Pal, U., Pal, S.K., Dasgupta, T.S., Ahmed, S.A., 2020. Unprecedented Regio- and Stereoselective Synthesis of Pyrene-Grafted Dispiro [indoline-3,2'-pyrrolidine-3',3'-indolines]: Expedient Experimental and Theoretical Insights into Polar [3 + 2] Cycloaddition. *ACS Omega*. 5, 24081–24094.
- Kamal, R.S., Migahed, M.A., Abd El-Sattar, N.E.A., 2022. Synthesis, characterization and performance of succinimide derivatives as anti-corrosion and anti-scalant in petroleum applications. *Journal of Molecular Liquids* 354, 118869.
- Kaur, M., Kumar, S., Younis, S.A., Yusuf, M., Lee, J., Weon, S., Kim, K.-H., Malik, A.K., 2021. Post-Synthesis modification of metal-organic frameworks using Schiff base complexes for various catalytic applications. *Chem. Eng. J.* 423, 130230.
- Khanna, R., Kalra, V., Kumar, R., Kumar, R., Kumar, P.R., Dahiya, H., Pahuja, P., Jha, G., Kumar, H., 2024. Synergistic experimental and computational approaches

- for evaluating pyrazole Schiff bases as corrosion inhibitor for mild steel in acidic medium. *Journal of Molecular Structure*. 1297, 136845.
- Kokalj, A., 2021. Molecular modeling of organic corrosion inhibitors: Calculations, pitfalls, and conceptualization of molecule–surface bonding. *Corrosion Science*. 193, 109650.
- Lemilemu, F., Bitew, M., Demissie, T.B., Eswaramoorthy, R., Endale, M., 2021. Synthesis, antibacterial and antioxidant activities of Thiazole-based Schiff base derivatives: a combined experimental and computational study. *BMC Chemistry*. 15, 67.
- Li, W.H., He, Q., Zhang, S.T., Pei, C.L., Hou, B.R., 2008. Some new triazole derivatives as inhibitors for mild steel corrosion in acidic medium. *J. Appl. Electrochem.* 38, 289–295.
- Li, Y., Zhong, H., Huang, Y., Zhao, R., 2019. Recent advances in AIEgens for metal ion biosensing and bioimaging. *Molecules*. 24, 4593.
- Long, J., 2019. Luminescent Schiff-base lanthanide single-molecule magnets: The association between optical and magnetic properties. *Front. Chem.* 7, 63.
- Mahadevi, P., Sumathi, S., 2020. Mini review on the performance of Schiff base and their metal complexes as photosensitizers in dye-sensitized solar cells. *Synth. Commun.* 50, 2237–2249.
- More, M.S., Joshi, P.G., Mishra, Y.K., Khanna, P.K., 2019. Metal complexes driven from Schiff bases and semicarbazones for biomedical and allied applications: a review. *Mater. Today Chem.* 14, 100195.
- Obot, I.B., Gasem, Z.M., 2014. Theoretical evaluation of corrosion inhibition performance of some pyrazine derivatives. *Corros. Sci.* 83, 359–366.
- Obot, I.B., Macdonald, D.D., Gasem, Z.M., 2015. Density functional theory (DFT) as a powerful tool for designing new organic corrosion inhibitors. Part I: An overview. *Corros. Sci.* 99, 1–30.
- Pour-Ali, S., Hejazi, S., 2022. Tiazofurin drug as a new and non-toxic corrosion inhibitor for mild steel in HCl solution: Experimental and quantum chemical investigations. *Journal of Molecular Liquids*. 354, 118886.
- Pour-Ali, S., Tavangar, R., Hejazi, S., 2023. Comprehensive assessment of some l-amino acids as eco-friendly corrosion inhibitors for mild steel in HCl: Insights from experimental and theoretical studies. *Journal of Physics and Chemistry of Solids*. 181, 111550.
- Priya, A.R.S., Muralidharam, V.S., Subramania, A., 2008. Development of novel acidizing inhibitors for carbon steel corrosion in 15% boiling hydrochloric acid. *Corrosion*. 64, 541–552.
- Rodríguez-Valdez, L.M., Villamizar, W., Casales, M., González-Rodríguez, J.G., Martínez-Villafañe, A., Martínez, L., Glossman-Mitnik, D., 2006. Computational simulations of the molecular structure and corrosion properties of amidoethyl, aminoethyl and hydroxyethyl imidazolines inhibitors. *Corros. Sci.* 48, 4053–4064.
- Stephens, P.J., Devlin, F.J., Chabalowski, C.F., Frisch, M.J., 1994. Ab initio calculation of vibrational absorption and circular dichroism spectra using density functional force fields. *J. Phys. Chem.* 98, 11623–11627.
- Uddin, M.N., Ahmed, S.S., Alam, S.M.R., 2020. REVIEW: Biomedical applications of Schiff base metal complexes. *J. Coord. Chem.* 73, 3109–3149.
- Verma, C., Quraishi, M.A., 2021. Recent progresses in Schiff bases as aqueous phase corrosion inhibitors: Design and applications. *Coord. Chem. Rev.* 446, 214105.
- Wahyuningrum, D., Achmad, S., Syah, Y.M., Buchari, B., Bundjali, B., Ariwahjoedi, B., 2008. The Correlation between Structure and Corrosion Inhibition Activity of 4,5-Diphenyl-1-vinylimidazole Derivative Compounds towards Mild Steel in 1% NaCl Solution. *Int. J. Electrochem. Sci.* 3, 154–166.
- Wysoglad, J., Ehlers, J.-E., Lewe, T., Dornbusch, M., Gutmann, J.S., 2018. Conformational study of melamine crosslinkers and spectroscopical comparison of HMMM molecules by practical measurements and quantum chemical calculations. *J. Mol. Struct.* 1166, 456–469.
- Xu, B., Yang, W.Z., Liu, Y., Yin, X.S., Gong, W.N., Chen, Y.Z., 2014. Experimental and theoretical evaluation of two pyridinecarboxaldehyde thiosemicarbazone compounds as corrosion inhibitors for mild steel in hydrochloric acid solution. *Corros. Sci.* 78, 260–268.
- Xu, B., Gong, W., Zhang, K., Yang, W., Liu, Y., Yin, X., Shi, H., Chen, Y., 2015. Theoretical prediction and experimental study of 1-Butyl-2-(4-methylphenyl)benzimidazole as a novel corrosion inhibitor for mild steel in hydrochloric acid. *J. Taiwan Inst Chem. E.* 51, 193–200.
- Yadav, M., Sarkar, T.K., Obot, I.B., 2016. Carbohydrate compounds as green corrosion inhibitors: electrochemical, XPS, DFT and Molecular Dynamics Simulation Studies. *RSC Adv.* 6, 110053–110069.
- Yurt, A., Duran, B., Dal, H., 2014. An experimental and theoretical investigation on adsorption properties of some diphenolic Schiff bases as corrosion inhibitors at acidic solution/mild steel interface. *Arabian Journal of Chemistry*. 7, 732–740.
- Zhang, K., Xu, B., Yang, W., Yin, X., Liu, Y., Chen, Y., 2015. Halogen-Substituted Imidazoline Derivatives as Corrosion Inhibitors for Mild Steel in Hydrochloric Acid Solution. *Corros. Sci.* 90, 284–295.